Supporting Information

Synthesis and structural characterization of the new Zintl phases $Eu_{10}Mn_6Bi_{12}$ and $Yb_{10}Zn_6Sb_{12}$

Ryan Janzen,[a, #] Sviatoslav Baranets,[a, #] Svilen Bobev [a,*]

[a] *Department of Chemistry and Biochemistry, University of Delaware, Newark, Delaware, 19716, United States.*
[b] *Department of Chemistry, Louisiana State University, Baton Rouge, LA 70803, United States.*

[#] *These authors contributed equally*
* Corresponding author Email: bobev@udel.edu.

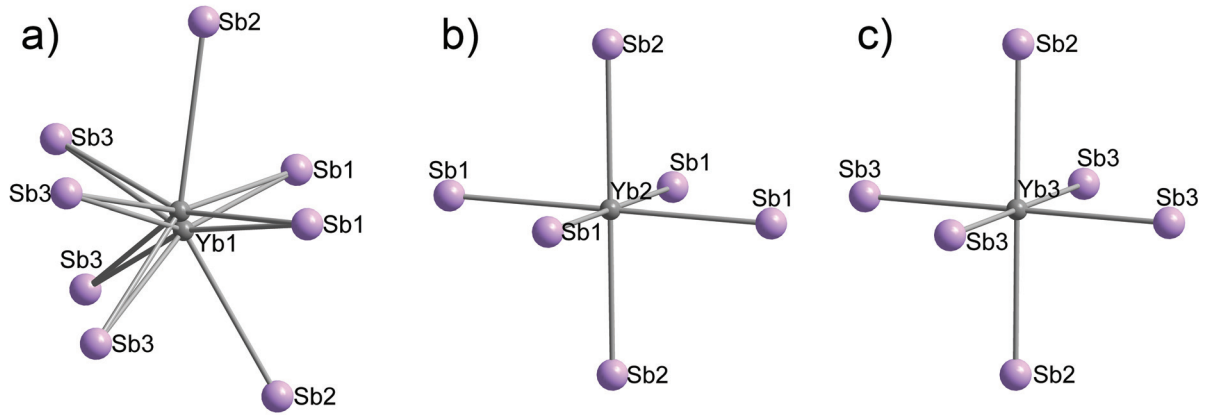

Figure S1. Cation coordination environments in $Yb_{10}Zn_6Sb_{12}$. As discussed in the text, Yb1 had very anisotropic displacement parameter (U_{11} was over 8 times larger than U_{22}), which suggested the possibility for a small positional disorder (4*i* site). By splitting this position to two 50% occupied 8*p* Wyckoff sites (approx. 0.4 Å apart), the shape of the ellipsoids was vastly improved. The 50% occupancy indicates the presence of only one Yb atom in the given position at a given time. All Yb-Sb distances are in normal ranges.

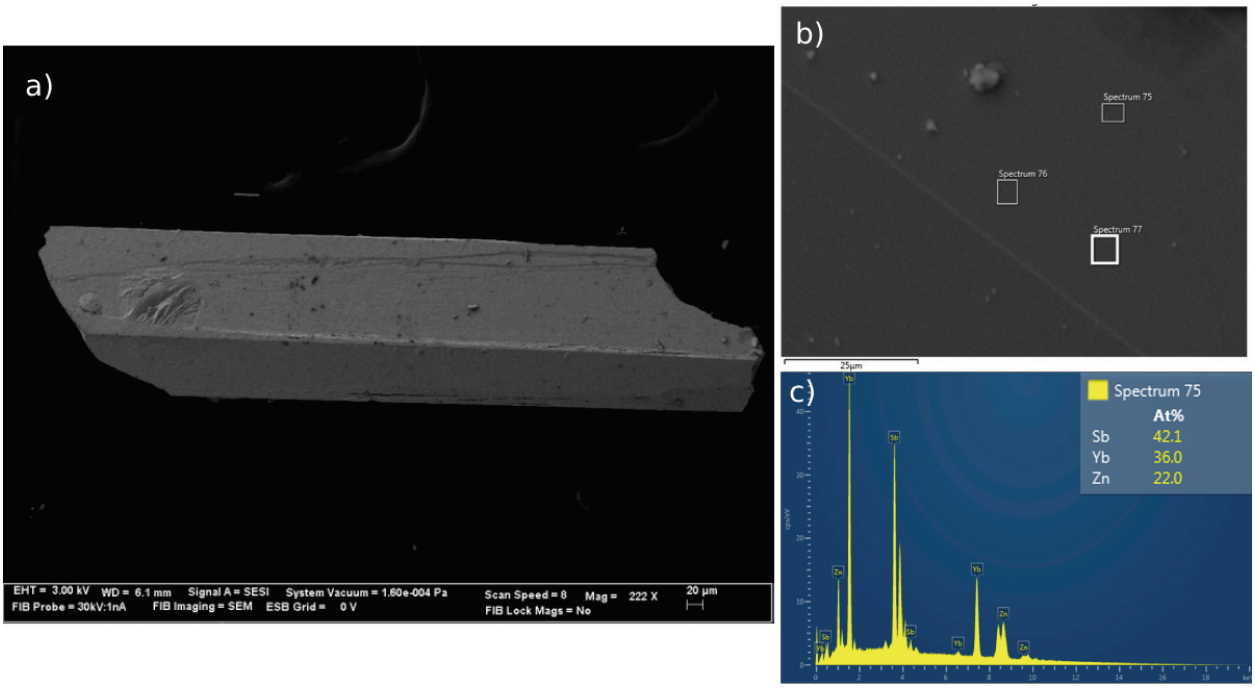

Figure S2. (a) SEM image of single-crystalline $Yb_{10}Zn_6Sb_{12}$. (b) Higher magnification SEM image of crystal, showing boxed EDX measurement sites. (c) Histogram from EDX analysis with measured atomic composition of crystal. Elemental analysis shows only three elements, and in the correct stoichiometric ratio.

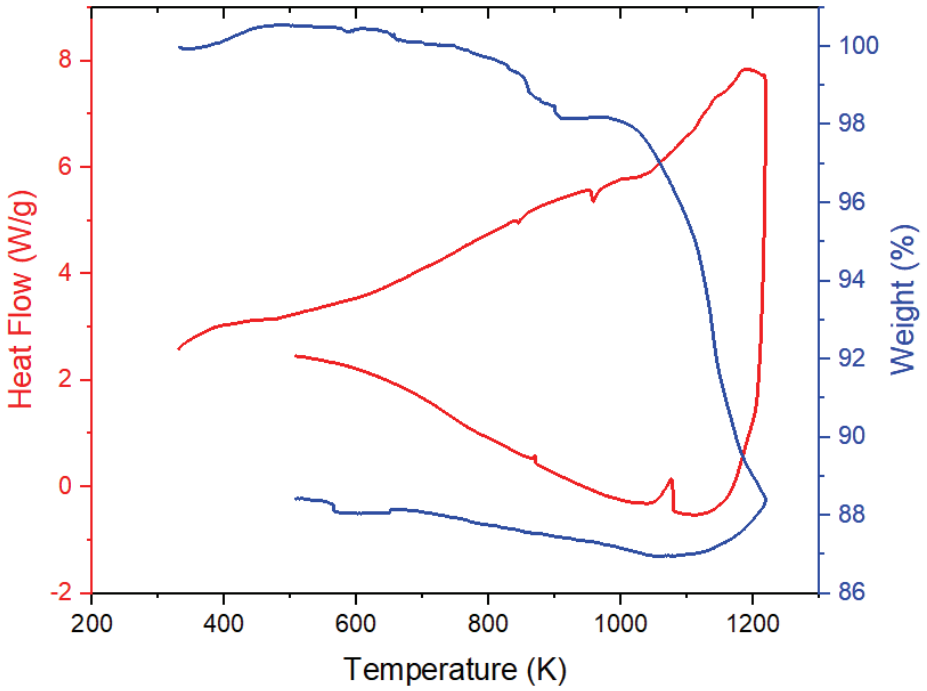

Figure S3. Combined TG-DSC analysis on single crystals of $Yb_{10}Zn_6Sb_{12}$. Weight% and specific heat flow are shown in blue and red, respectively.

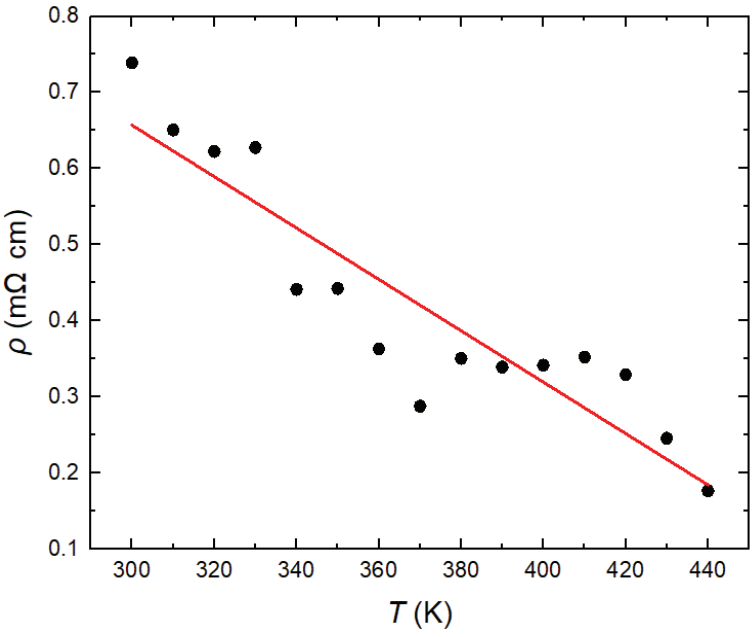

Figure S4. Temperature dependence of the resistivity for $Yb_{10}Zn_6Sb_{12}$. Each point is an average of the consistent measurements at that temperature. A linear fit is included to illustrate the trend.

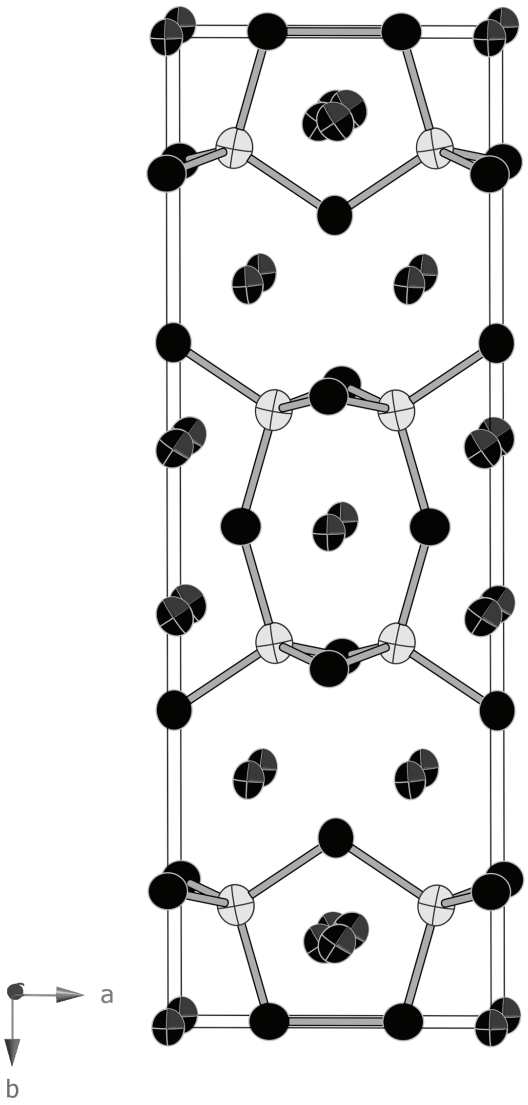

Figure S5. Structural representation for $Yb_{10}Zn_6Sb_{12}$ with anisotropic displacement parameters, drawn at the 98% probability level.

Results from refinements of the $Eu_{10}Mn_6Bi_{12}$ structure with split Eu1 position.

Unlike the $Yb_{10}Zn_6Sb_{12}$ structure where there was a significant elongation of the Yb1 thermal parameter and some residual features on the difference Fourier map (peak and hole near Yb1), in the $Eu_{10}Mn_6Bi_{12}$ structure, the Eu1 anisotropic displacement parameter is much more uniform (U_{11} is ca. 2.5 times larger than U_{22}). Attempts to refine a model with split Eu1 on two 8*p* Wyckoff sites did not yield statistically significant improvements. Below is a summary of those trial refinements

$Yb_{10}Zn_6Sb_{12}$
Yb1 at 4*i*

Yb1	U_{11}	U_{22}	U_{33}	U_{23}	U_{13}	U_{12}
	0.0641(6)	0.0087(4)	0.0125(3)	0	0	0

residual peak & hole: 3.85/-4.88
R_1 = 0.0297 ($I \geq 2\sigma_I$)
wR_2 = 0.0634 ($I \geq 2\sigma_I$)

Yb1 at 8*p*

Yb1	U_{11}	U_{22}	U_{33}	U_{23}	U_{13}	U_{12}
	0.027(2)	0.0125(3)	0.0162(3)	0	0	-0.0035(4)

residual peak & hole: 1.53/-2.27
R_1 = 0.0250 ($I \geq 2\sigma_I$)
wR_2 = 0.0545 ($I \geq 2\sigma_I$)

$Eu_{10}Mn_6Bi_{12}$
Eu1 at 4*i*

Eu1	U_{11}	U_{22}	U_{33}	U_{23}	U_{13}	U_{12}
	0.057(1)	0.0222(8)	0.0253(9)	0	0	0

residual peak & hole: 2.37/-2.20
R_1 = 0.0353 ($I \geq 2\sigma_I$)
wR_2 = 0.0637 ($I \geq 2\sigma_I$)

Eu1 at 8*p*

Eu1	U_{11}	U_{22}	U_{33}	U_{23}	U_{13}	U_{12}
	0.020(5)	0.0225(8)	0.0258(9)	0	0	-0.003(1)

residual peak & hole: 2.41/-2.04
R_1 = 0.0349 ($I \geq 2\sigma_I$)
wR_2 = 0.0624 ($I \geq 2\sigma_I$)

Based on the above, $Yb_{10}Zn_6Sb_{12}$ structure is presented with Yb1 located at 8*p* (50%) and the $Eu_{10}Mn_6Bi_{12}$ structure is presented with Eu1 located at 4*i*